INEXPENSIVE SENSING FOR FULL STATE ESTIMATION OF SPACECRAFT

B. Pigneur[1]*, K. Ariyur[2]

[1]Graduate Student, Mechanical Engineering, Purdue University, USA
[2]Professor, Mechanical Engineering, Purdue University, USA

ABSTRACT

This paper is a preliminary study of a new method of full state estimation in order to increase spacecraft autonomy. Autonomous systems help to reduce costs during the operational lifetime and improve spacecraft capabilities when human interaction is limited. The proposed method is based on low SWAP (size, weight, and power) sensing elements. The relation between the numbers and the location on the space vehicle of these devices are keys to the proposed technique. This paper presents the advantage of this technique in several simple scenarios. It also lays down the path to consolidate this theory with more in-depth studies.

Key words: sensor; measurement; MEMS accelerometer; inertia estimation; autonomous guidance and control; entry, descent and landing system.

1. INTRODUCTION

Over the years, several autonomous control algorithms have been studied and developed for space exploration and planetary or asteroid landing. Starting with the apollo program with gravity turn manoeuvre and profile tracking ('Moseley 1969'). Similar principles of tracking specific profiles and variables have been studied and used since ('Lu & Bayard '). Recently, several guidance and control algorithms have been developed such as terminal point controller ('Mendeck & Carmin 2002'), numerical predictor-corrector and analytical predictor-corrector ('Davis et al. 2010'), powered-descent guidance based on Apollo Lunar Module guidance ('Sostaric & Rea 2005') and convex optimization of powered-descent guidance ('Carson et. al 2011'). These techniques rely on accurate knowledge of state variables. Improvements of measurement accuracy and autonomous algorithms are beneficial. For example, future crewed mission to Mars will require improvement in landed mass and precision landing. In particular inflatable aerodynamic decelerators (IAD) and supersonic retropropulsion (SRP) have been extensively studied ('Braun & Manning 2009', 'Davis et al. 2010' and 'Sostaric et al. 2011'). This requires accurate knowledge of the spacecraft state variables. One way to control the lift and drag of IAD is by controlling the displacement of its center of mass. Again, accurate knowledge of the state estimation is determinant to the development of these control algorithms.

At the Autonomous Systems Laboratory at Purdue University, we believe that the autonomy of a spacecraft can be dramatically improved by direct measurements of the full state. This paper starts with the premise that better measurements will improve the autonomy of the GNC algorithms. Mathematical theory for accelerometer based IMU (inertial measurement unit) has been studied by 'Gullipalli & Ariyur 2011'. The method we propose refers to the mathematical theory developed in this cited paper.

One of the purpose of autonomy is ultimately to reduce the costs of these vehicles during their operational life. To that end, we choose to use inexpensive, low SWAP (size, weight, and power) sensing elements, such as MEMS accelerometers on every moving part in the space vehicle. The novelty does not reside in the development of new costly instruments but in a different way to exploit well characterized, light-weight, and inexpensive sensors. Through the use of multiple accelerometers, we are able to obtain a broader range of measurements, and thus greater information on the state of the vehicle. In this paper we lay emphasis on the estimation of the real time variation of the inertia, the mass and the center of mass of the spacecraft by measurement of accelerations. Then we analyse its effects on the autonomous control algorithms of the spacecraft.

2. METHODOLOGY

Spacecraft are subject to the space environment. Gravity, solar pressure, ionic wind and atmosphere are some of the disturbances that affect the dynamics of a spacecraft. In order to increase autonomy and reduce human interactions, the spacecraft should rely on accurate knowledge of its dynamics state. We choose to measure several accelerations because of their connection to the state, and the availability of low SWAP sensors for its measurement. A better estimation of the acceleration leads in a better estimation of the position of the spacecraft. A classical

*bpigneur@purdue.edu

way to measure the acceleration is by use of an IMU (Inertial Measurement Unit) and accurate accelerometer. Instead of trying to develop better and heavier instruments, a combination of small, cheap and light accelerometers can give us a better estimation of the acceleration of a spacecraft.

MEMS accelerometers are small, cheap and light such as the one used in almost every smartphone. Of course these types of accelerometers are not very accurate nor reliable. A single MEMS accelerometer is clearly not enough but a combination of several of these devices can be advantageous. Due to the large number of those, the estimation of the acceleration is not affected in case of inaccuracy or dysfunction of some of the sensors.

The large number of these devices allows to cover different parts of the space vehicle. Depending on the spacecraft's configuration and the scenario, deployable and moving parts can play a significant role in the dynamics behavior of the spacecraft. Small and light MEMS accelerometers can be dispersed across those flexible parts and provide useful information. A key factor is the relation between the positions of the devices d_i and the measurements of acceleration a_i. The equations 1 and 2 represent the estimation of the linear acceleration $a_{estimated}$ and the angular acceleration $\alpha_{estimated}$ (where n is the number of devices). Both the linear and the angular accelerations can be estimated with high accuracy from the acceleration measurements and their geometric configuration.

$$a_{estimated} = f(a_1, ..., a_n, d_1, ..., d_n) \tag{1}$$
$$\alpha_{estimated} = g(a_1, ..., a_n, d_1, ..., d_n) \tag{2}$$

The simplest method is to take the average value of these accelerations without looking at the location of the devices (equation 3). This improves the measured value of the acceleration but since the accuracy of these cheap devices is not very good, the error between the estimated and the measured value is still significant.

$$a_{estimated} = \frac{\Sigma_{i=1}^{n} a_i}{n} \tag{3}$$

Different methods combining acceleration measurements and location of these devices give better results. The distance between the locations of the different measurement units (leverage arm) is important. If all devices are clustered in one area, the calculation of the acceleration wont be as accurate as if the leverage arm was bigger. A more spread out configuration gives better results. The method should integrate this factor. A simple example is given by the equation 4.

$$a_{estimated} = \frac{f(a, d)}{g(d)} \tag{4}$$

More advance techniques are described in 'Gullipalli & Ariyur 2011'. Let us start with a simple configuration of four three-axis accelerometers located at each corner of a square. The acceleration equation can be obtained from Newton's second law of motion with inertial to non-inertial frame conversion formula with constant mass (equation 5).

$$\frac{d^2 r}{dt^2} = \frac{d^2 R}{dt^2} + \omega \times \omega \times r' + 2\omega \times \frac{dr'}{dt} + \alpha \times r' \tag{5}$$

R is the distance in the inertial frame, r' is the distance in the non-inertial frame (rotating frame), ω is the angular velocity and α is the angular acceleration. Then the acceleration equations can be expressed as follow (equations 6 to 8):

$$A_{ix} = a_x - (\omega_y^2 + \omega_z^2) r_{xi} + \omega_x \omega_y r_{yi} + \omega_x \omega_z r_{zi} + \alpha_y r_{zi} - \alpha_z r_{yi} \tag{6}$$
$$A_{iy} = a_y - (\omega_x^2 + \omega_z^2) r_{yi} + \omega_x \omega_y r_{xi} + \omega_y \omega_z r_{zi} + \alpha_z r_{xi} - \alpha_x r_{zi} \tag{7}$$
$$A_{iz} = a_z - (\omega_x^2 + \omega_y^2) r_{zi} + \omega_x \omega_z r_{xi} + \omega_y \omega_z r_{yi} + \alpha_x r_{yi} - \alpha_y r_{xi} \tag{8}$$

The subscript i represents the index of the measurement units. a_x, a_y, a_z are the linear accelerations of the body in the x,y,z directions, r_{xi}, r_{yi}, r_{zi} are the ith accelerometer positions in the x,y,z directions, $\omega_x, \omega_y, \omega_z$ are the components of the angular velocity of the body along the 3 axes and $\alpha_x, \alpha_y, \alpha_z$ are the components of the angular acceleration of the body along the 3 axes. Finally A_{ix}, A_{iy}, A_{iz} are the i^{th} accelerometer measurement in the x,y,z directions. These equations show the relation between the linear acceleration, the angular velocity, the angular acceleration and the position of the accelerometers.

The linear equations of the product of the pair of the angular velocities are obtained by eliminating the angular accelerations and the second order terms of the equations 6 to 8. These linear equations are:

$$(r_{12x} r_{34y} - r_{34x} r_{12y}) \omega_x \omega_y + (r_{12x} r_{34z} - r_{34x} r_{12z}) \omega_x \omega_z = r_{12x} A_{34x} - r_{34x} A_{12x} \tag{9}$$
$$(r_{41z} r_{23y} - r_{23z} r_{41y}) \omega_y \omega_z + (r_{41x} r_{23y} - r_{23x} r_{41y}) \omega_x \omega_y = r_{41y} A_{23y} - r_{23y} A_{41y} \tag{10}$$
$$(r_{13x} r_{42z} - r_{42x} r_{13z}) \omega_x \omega_z + (r_{13y} r_{42z} - r_{42y} r_{13z}) \omega_y \omega_z = r_{13z} A_{42z} - r_{42z} A_{13z} \tag{11}$$

The numerical subscripts $1, 2, 3, 4$ identify the accelerometers.

We propose to investigate several methods in order to optimize the accuracy of the technique by minimizing the error between the measured and the estimated acceleration. Not only this method includes the location of the devices but also detects outlier measurements (in case of failing devices) and excludes them from the calculation of the acceleration.

In order to drastically improve the state estimation, a good mapping of the spacecraft is necessary. The knowledge of the numbers and the location of these devices are key factors used in this methodology.

In addition, another factor that plays a part in the position and the attitude of a spacecraft, is the change of its inertia. Euler equations of motion (equations 12, 13 and 14) established a relation between inertia and angular acceleration. The kinematic equations (equations 15, 16 and 17) linked the angular velocity to the attitude of a spacecraft. So accurate knowledge of the inertia of the space vehicle is beneficial to the determination of the spacecraft attitude.

$$\dot{\omega_x} = \frac{M_x}{I_x} - \frac{(I_x - I_y)}{I_x}\omega_y\ \omega_z \tag{12}$$

$$\dot{\omega_y} = \frac{M_y}{I_y} - \frac{(I_x - I_z)}{I_y}\omega_x\ \omega_z \tag{13}$$

$$\dot{\omega_z} = \frac{M_z}{I_z} - \frac{(I_y - I_x)}{I_z}\omega_x\ \omega_y \tag{14}$$

$$\dot{\phi} = \omega_x + (\omega_y\ sin\phi + \omega_z\ cos\phi)\ tan\theta \tag{15}$$

$$\dot{\theta} = \omega_y\ cos\phi - \omega_z\ sin\phi \tag{16}$$

$$\dot{\psi} = (\omega_y\ sin\phi + \omega_z\ cos\phi)\ \frac{1}{cos\theta} \tag{17}$$

Similarly to the method used for acceleration estimation, MEMS accelerometers are displayed on every moving parts or other pieces responsible for a change of inertia. Measurement of the change of acceleration of these parts with respect to the center of mass of the space vehicle, leads to an accurate estimation of the displacement of significant masses. So the inertia of the vehicle can be estimated as well. Then we can actively use the change of inertia to control the attitude of the spacecraft.

3. MEASUREMENTS UNITS

Several sensing elements can be considered. The goal is to reduce the weight, size and power requirement. This paper investigates MEMS accelerometers. They are small cheap, light-weight and commonly used in several applications. The method proposed is not limited to accelerometer but can be applied to other sensing devices. CMOS imagers dispersed on the outer surface of the vehicle are another example of elements that can be used to replace expensive star-tracker. This paper focus on acceleration estimation but the proposed method is not limited to this variable.

4. TEST CASES

Several test cases are described in the following sections in order to illustrate the benefice of this technique. First, a scenario of a simple circular orbit around the Moon is presented (section 4.1.). Then a Moon descent and landing scenario is discussed (section 4.2.). Finally, the advantage of this method is applied to spacecraft's inertia estimation (section 4.3.).

These simulations are preliminary results that allow us to demonstrate the advantage of a better estimation of the acceleration with respect with traditional IMU measurement.

4.1. Moon Circular Orbit

The first scenario used to illustrate the advantage of this method is a simple planar circular orbit around the Moon. This simple case has been selected to validate the method. Standard IMU sensing and Multi-Sensors MEMS accelerometers are compared to a nominal case (perfect measurement of the acceleration). The Standard IMU is a more accurate sensing unit (1% dispersion on the nominal acceleration) than each of the MEMS accelerometers (5% dispersion on the nominal acceleration). We choose different accuracy to reflect that the quality of the MEMS sensing elements is not the main factor of the improvement of the estimation.

The trajectories (one orbit revolution) of the Nominal Case, the Standard IMU Case and the Multi-Sensors Case are presented in the figure 1. This figure illustrates that both configurations are close to the nominal trajectory. None of them significantly perturbs the orbit over one period in a way that the shape is dramatically changed. Nevertheless there are some perturbations that can be observed in the figure 2.

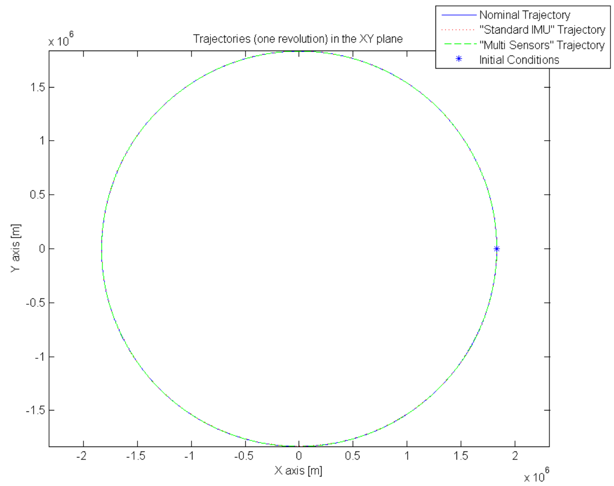

Figure 1. XY orbital plane.

These dispersions of the trajectory after one orbital period can better be observed in the figure 2. This figure shows the altitude of the vehicle. It is observable that the Multi-Sensors technique gives a relatively better estimation of the trajectory.

The figure 3 presents the dispersion ellipse after one orbital period. Significant improvement can be ob-

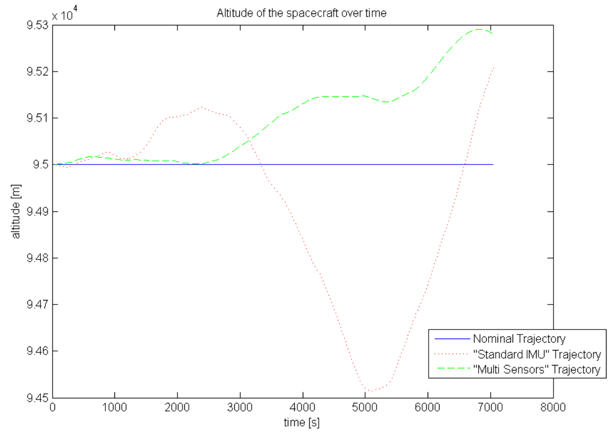

Figure 2. Altitude of the spacecraft.

served with the proposed Multi-Sensors method. The use of a combination of multiple MEMS accelerometers drastically reduces the dispersion due to error in acceleration estimation. This illustrates that even if the Standard IMU as a better accuracy (1% dispersion on measurement) than each individual MEMS accelerometer (5% dispersion on measurement), the error in the estimation of acceleration is bigger. The advantage of the new method is visible on the figure 3. Note that with similar accuracy, the advantage of the Multi-Sensors technique is even better.

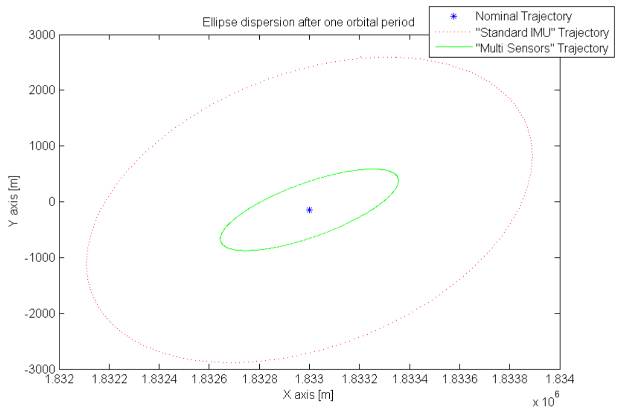

Figure 3. Dispersion Ellipse after one orbital period.

4.2. Moon Descent and Landing

The second test case is a simple descent and landing scenario. Moon environment has been selected to avoid atmospheric disturbances and validate the new technique in a propulsive landing. The goal is to observe the advantage and the behavior of the proposed method in a scenario where the dynamics changes more quickly than the previous test case.

The initial conditions are an altitude of 95 km with a velocity magnitude of 1670 m/s and a flight path angle of -10deg.

The figure 4 shows the estimation of the acceleration along the X-axis. One can observe that the new method reduce the dispersion of the acceleration measurement. Similar observation can be done about the other axis.

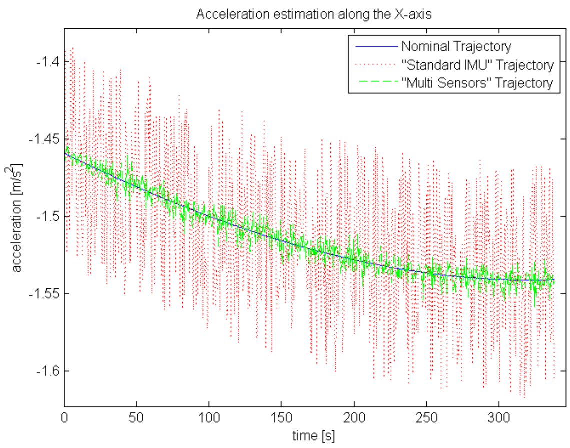

Figure 4. Acceleration estimation along X-axis.

The figure 5 represents the landing dispersion ellipses of both the Standard IMU and Multi-Sensors simulation. As in the Circular Test Case (section 4.1.), the dispersion is significantly reduced. The figure represents the worst case scenario of both techniques. A dispersion of 5% of the measured acceleration has been considered in this example. Smaller percentage values reduce the dispersion ellipses but the relation between Standard IMU and multiple MEMS accelerometers is not significantly affected.

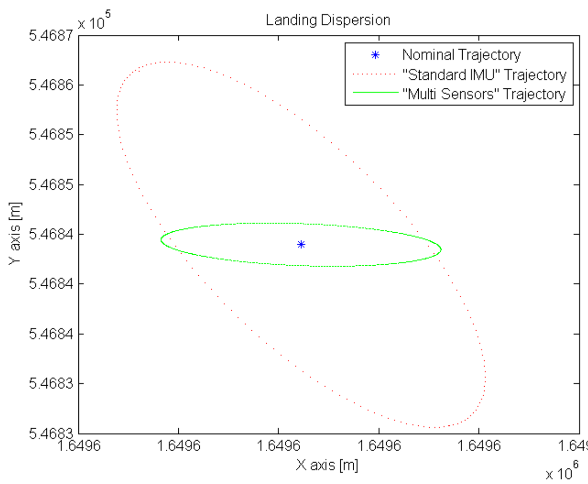

Figure 5. Landing dispersion ellipse.

4.3. Effects on Spacecraft Inertia

As presented in section 2., the inertia affects the angular acceleration and thus the attitude of the spacecraft. This case is based on the same initial conditions as in section 4.2.

The spacecraft is single-axis stabilized along the main component of the thrust direction and the direction of one of the principal moment inertia. The effect of the inertia estimation is observed on the others principal moment of inertia axis. After 200 seconds, an external torque (due to thruster activation) acts on the space vehicle for 70 seconds. No other control (except that inertia control) is applied so the effect of inertia estimation can be directly observed.

The figure 6 represents one of the perpendicular angular acceleration components. The on and off switches of the thruster are visible at 200 seconds and 270 seconds. The graph on the top shows a nominal simulation with constant inertia. The bottom graph represents the simulation with Multi-Sensors inertia estimation. On the top graph, we can see the effects of no active control. By comparison, the bottom graph shows that small displacements of masses affects the inertia and can compensate the perturbing angular acceleration.

The figure 7 illustrates the impact of the angular acceleration on one of the Euler Angles. It is observable that during the thrusting time, the Euler Angle is not controlled. This is because we are observing the spacecraft behavior along uncontrolled/unstable axis. More study has to be done to demonstrate the impacts of this estimation method on 3-axis stabilized spacecraft.

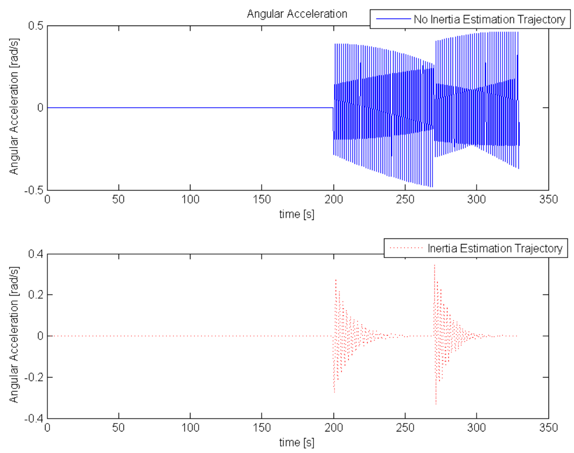

Figure 6. Angular Acceleration.

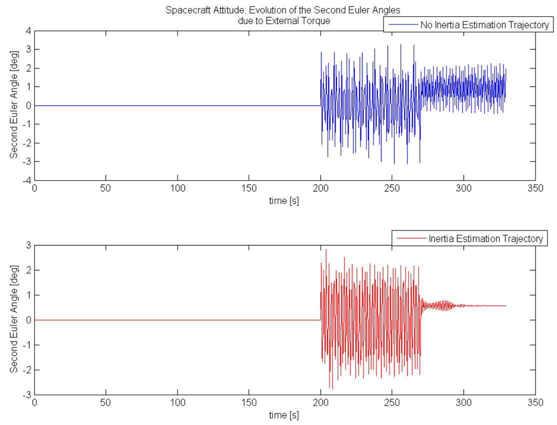

Figure 7. Second Euler Angle.

5. FUTURE WORK AND CONCLUSION

Several simple test cases have been presented in this paper to illustrate the advantages of the proposed method for spacecraft full state estimation. This paper focused on MEMS acccelerometers devices and their contribution to a better knowledge of spacecraft state estimation. As illustrated, better estimation of the acceleration vector is useful toward autonomous control and ultimately toward cost reduction. Not only low SWAP (size, weight and power) sensing elements will reduce the manufacturing cost but they will also reduce the cost due to station keeping in the case of extended operational life. It will also be beneficial in cases where human interactions are limited such as entry, descent and landing scenario as illustrated in section 4.2.

Future work would be to apply this technique in more challenging environment such as atmospheric entry in order to test the robustness of the method. There are still questions to be answered such as: How low can be the quality of the MEMS accelerometers and still gives better estimation than traditional IMU? What is the best geometric configuration? What is the maximum gain in accuracy? Future work will help to improve the determination of the optimal relation between the number of sensing elements, the location of these devices and the impact on the autonomous GNC.

More work has to be done to demonstrate the advantage of this new estimation technique on attitude control of space vehicles. So far only simple simulations allow us to see the potential impact of such method.

A more in depth study on the cost reduction can also be done. New GNC algorithms will be developed to fully take advantage of this new technique and maximize the potential of this method.

This technique can be applied not only to accelerometers but also to different measurement units such as CMOS camera or other devices designed to track the Sun and stars. This will allow us to better estimate the position and the attitude of the spacecraft.

REFERENCES

Braun, R., Manning R. 2009, Mars Exploration Entry, Descent and Landing Challenges, IEEAC paper 0076

Davis, J., Dwyer Cianciolo, A.,Powell, R., Schidner, J., Garcia-Llama, E. 2010, Guidance and Control Algorithms for the Mars Entry, Descent and Landing Systems Analysis, Proceedings of the 2010 AIAA/AAS Specialist Conference, AIAA 2010-7972-287, Toronto, Canada, August 2010

Moseley, P. 1969, The Apollo Entry Guidance: A Review of the Mathematical Development and Its Operational Characteristics, TRW note no 69-FMT-791

Boussalis, D. 1996, Investigation of Longitudinal Motion of Low-Lift Entry Vehicles, JPL Engineering Memorandum No. 3456-96-002

Lu, W.M., Bayard, D., Guidance and Control for Mars Atmospehric Entry: Adaptativity and Robustness

Sostaric, R., Zumwalt, C., Garcia-Llama, E., Powell, R., Schidner, J. 2011, Trajectory Guidance for Mars Robotic Precursors: Aerocapture, Entry, Descent and Landing, Proceedings of the 2011 International Planetary Probe Workshop

Ljung, L. 1987, System Identification: Theory for the User, P T R Prentice Hall

Gullipalli, P., Ariyur, K. 2011, Acceleromter Dased Inertial Measurement Units, Proceeding of the ION International Technical Meeting, San Diego, CA, USA, January 2011.

Mendeck, G., Carman, G. 2002, Guidance Design for Mars Smart Landers Using The Entry Terminal Point Controller, Proceeding of the AIAA Atmospheric Flight Mechanic Conference and Exhibit, Monterey, CA, USA, August 2002.

Sostaric, R., Rea, J. 2005, Power Descent Guidance Methods For The Moon And Mars, Proceeding of the AIAA Guidance Navigation and Control Conference and Exhibit, San Francisco, CA, USA, August 2005.

Carson, J., Acikmese, B., Blackmore, L. 2011, Lossless Convexification of Power-Descent Guidance with Non-Convex Thrust Bound and Pointing Constraints, Proceeding of the American Control Conference, San Francisco, CA, USA, June-July 2011.